Ab Initio Molecular Dynamics Calculations of the Phase Transformation Mechanism for the Formation of TiO_2 Titanate-Type Nanosheets from Anatase

Fernando Alvarez-Ramirez* and Yosadara Ruiz-Morales

Programa de Ingeniería Molecular, Instituto Mexicano del Petróleo, Eje Central Lázaro Cárdenas 152, México, Distrito Federal, 07730, México

Received September 11, 2006. Revised Manuscript Received March 20, 2007

This work investigates the transformation mechanism, at atomic level, of anatase to titanate-type structures by carrying out ab initio molecular dynamics (ab-MD) calculations with the Harris functional, including the Γ-point approximation and also several *k*-points. The transformation mechanism is presented and discussed. Three different size wire models of anatase with periodic conditions along the (0,1,0) direction were used, and several different environment conditions were investigated. It is found that the titanate-type structure is energetically favorable. The transformation was followed by monitoring the formation of four-coordinated oxygen atoms, which constitute the characteristic sequence of edge-sharing TiO_6 octahedrons of titanates. Additionally, the titanate-type structure can be transformed to anatase in a reverse mechanism. A very important factor in the transformation of the anatase-type sections to the TiO_6 octahedrons is the interaction of the $(0,0,\pm1)$ surfaces of the anatase with positive charges (Na^+), which stress the surface deforming it and promoting the transformation.

1. Introduction

Titanium oxide is commonly found as a three-dimensional structural material (3D), and it is mainly used in heterogeneous catalysis, as photocatalyst, in solar cells for the production of hydrogen and electric energy, as gas sensor, as white pigment (e.g., in paints and cosmetic products), as corrosion-protective coating, as optical coating, in ceramics, and in electric devices such as varistors.[1]

Titanium dioxide is known to exist in three crystalline phases: anatase, rutile, and brookite as well as in an amorphous phase. There are other phases but these are the most common. The anatase and rutile phases have a tetragonal crystal lattice while the brookite has an orthorhombic lattice. It has been reported that at elevated pressures TiO_2 has a rich phase diagram with a series of structural phase transformations.[2]

It is reported in the literature that the hydrothermal treatment or chemical treatment of anatase in NaOH, with or without a subsequent acid wash, produces nanostructures that include nanosheets, nanobelts, nanoribbons, and nanotubes.[3−31] Furthermore, several different crystalline phases have been proposed to be the building unit in these nanostructures. On one hand, anatase has been reported as the building unit;[3−10,12] on the other hand, the following titanate structures have been proposed as the unit cell: Na_2-

* To whom correspondence should be addressed. E-mail: falvarez@imp.mx.

(1) Diebold, U. *Surf. Sci. Rep.* **2003**, *48*, 53.
(2) Muscat, J.; Swamy, V.; Harrison, N. M. *Phys. Rev. Lett.* **2002**, *65*, 224112.
(3) Kasuga, T.; Hiramatsu, M.; Hoson, A.; Sekino, T.; Niihara, K. *Langmuir* **1998**, *14*, 3160.
(4) Kasuga, T.; Hiramatsu, M.; Hoson, A.; Sekino, T.; Niihara, K. *Adv. Mater.* **1999**, *11*, 1307.
(5) Seo, D. S.; Lee, J. K.; Kim, H. *J. Cryst. Growth* **2001**, *229*, 428.
(6) Zhu, Y.; Li, H.; Koltypin, Y.; Hacohen, Y. R.; Gedanken, A. *Chem. Commun.* **2001**, 2616.
(7) Zhang, Q.; Gao, L.; Sun, J.; Zheng, S. *Chem. Lett.* **2002**, 226.
(8) Wang, Y. Q.; Hu, G. Q.; Duan, X. F.; Sun, H. L.; Xue, Q. K. *Chem. Phys. Lett.* **2002**, *365*, 427.
(9) Yao, B. D.; Chan, Y. F.; Zhang, X. Y.; Zhang, W. F.; Yan, Z. T.; Wang, N. *Appl. Phys. Lett.* **2003**, *82*, 281.
(10) Tsai, C. C; Teng, H. *Chem. Mater.* **2004**, *16*, 4352.
(11) Tsai, C. C; Teng, H. *Chem. Mater.* **2006**, *18*, 367.
(12) Wang, W.; Varghese, O. K.; Paulóse, M.; Grimes, C. A. *J. Mater. Res.* **2004**, *19*, 417.
(13) Yang, J.; Jin, Z.; Wang, X.; Li, W.; Zhang, J.; Zhang, S.; Guo, X.; Zhang, Z. *J. Chem. Soc., Dalton Tans.* **2003**, *20*, 3898.
(14) Zhang, M.; Jin, Z.; Zhang, J.; Guo, X.; Yang, J.; Li, W.; Wang, X.; Zhang, Z. *J. Mol. Catal. A: Chem.* **2004**, *217*, 203.
(15) Du, G. H.; Chen, Q.; Che, R. C; Yuan, Z. Y.; Peng, L. M. *Appl. Phys. Lett.* **2001**, *79*, 3702.
(16) Chen, Q.; Du, G. H.; Zhang, S.; Peng, L. M. *Acta Crystallogr., Sect. B* **2002**, *58*, 587.
(17) Chen, Q.; Zhou, W. Z.; Du, G. H.; Peng, L. M. *Adv. Mater.* **2002**, *14*, 1208.
(18) Tian, Z. R.; Voigt, J. A.; Liu, J.; Mckenzie, B.; Xu, H. *J. Am. Chem. Soc.* **2003**, *725*, 12384.
(19) Zhang, S.; Peng, L.-M.; Chen, Q.; Du, G. H.; Dawson, G.; Zhou, W. Z. *Phys. Rev. Lett.* **2003**, *91*, 256103.
(20) Sun, X.; Li, Y. *Chem.−Eur. J.* **2003**, *9*, 2229.
(21) Yuan, Z.-Y.; Su, B.-L. *Colloids Surf., A* **2004**, *241*, 173.
(22) Thorne, A.; Kruth, A.; Tunstall, D.; Irvine, J. T. S.; Zhou, W. *J. Phys. Chem. B* **2005**, *709*, 5439.
(23) Zhang, S.; Chen, Q.; Peng, L.-M. *Phys. Rev. B* **2005**, *71*, 014104.
(24) Nakahira, A.; Kato, W.; Tamai, M.; Isshiki, T.; Nishio, K. *J. Mater. Sci.* **2004**, *39*, 4239.
(25) Ma, R.; Bando, Y.; Sasaki, T. *Chem. Phys. Lett.* **2003**, *380*, 577.
(26) Ma, R.; Fukuda, K.; Sasaki, T.; Osada, M.; Bando, Y. *J. Phys. Chem. B* **2005**, *109*, 6210.
(27) Fukuda, K.; Nakai, I.; Oishi, C.; Nomura, M.; Harada, M.; Ebina, Y.; Sasaki, T. *J. Phys. Chem. B* **2004**, *108*, 13088.
(28) Sakia, N.; Ebina, Y.; Takada, K.; Sasaki, T. *J. Am. Chem. Soc.* **2004**, *126*, 5851.
(29) Sasaki, T.; Ebina, Y.; Tanaka, T.; Harada, M.; Watanabe, M. *Chem. Mater.* **2001**, *13*, 4661.
(30) Sasaki, T.; Watanabe, M. *J. Phys. Chem. B* **1997**, *101*, 10159.
(31) Yuan, Z.-Y.; Colomer, J.-F.; Su, B.-L. *Chem. Phys. Lett.* **2002**, *363*, 362.

10.1021/cm062162l CCC: $37.00
Published on Web 05/18/2007

$Ti_2O_5 \cdot H_2O$ or $H_2Ti_2O_5 \cdot H_2O$,[13,14] $Na_2Ti_3O_7$ or $H_2Ti_3O_7$,[15−23] $H_2Ti_4O_9 \cdot H_2O$,[24] and lepidocrocite-type titanate structure.[25−30,32] Also, TiO_2(B) has been proposed as the construction unit of the TiO_2 nanostructures.[33] Wang et al.[8] have proposed a mechanism of formation of TiO_2 nanotubes that are produced during the hydrothermal treatment in NaOH, which involves the exfoliation of anatase layers or sheets from the starting anatase bulk, followed by the rolling of the sheets into scrolls. However, it is not clear in the literature how the exfoliation mechanism takes place.

In the literature, there are reported several synthesis-schematic diagrams of the transformation between the different titanates and polymorphs of TiO_2 during hydrothermal treatment in NaOH and subsequent treatments.[34−43] Many groups have tried to modify the process and have tried to elucidate the mechanism of formation as well as the true composition and crystalline structure of the resulting titania nanostructures. There is a common agreement that after breaking chemical bonds of the starting three-dimensional TiO_2 structure, planar entities are formed. Bavykin et al.[42] proposed a mechanism of formation of nanotubes which schematically comprises the following steps: (a) dissolution of TiO_2 precursor, (b) dissolution−recrystallization of nanosheets, (c) curving of nanosheets, and (d) washing of nanotubes. The mechanism that explains, at atomic level, how the anatase is transformed into titanates, or lepidocrocite-type titanate, or how it keeps its anatase structure (in the exfoliated nanosheet) during the so-called "dissolution−recrystallization" step b in Bavykin's mechanism has not been clarified. Therefore, the aim of this paper is to shed light on the transformation mechanism, at atomic level, of anatase to titanates and lepidocrocite-type titanate structure and to elucidate the effect of the size of the initial anatase crystal and the presence of NaOH during the hydrothermal treatment by carrying out ab initio molecular dynamics (ab-MD) calculations of anatase crystalline wires of different sizes.

2. Computational Details

As initial configuration, we selected periodic anatase-type wire sections of different sizes to investigate the size dependence on the structural transformation. In Figure 1a, 1c, and 1e, the three different size anatase-type wire models ($Ti_8O_{18}H_4$, $Ti_{18}O_{40}H_8$, and $Ti_{28}O_{62}H_{12}$, respectively), that we used in the calculations, are shown. As it can be seen in Figure 1a, 1c, and 1e, all the models have approximately the same length, ∼15 Å, in the (1,0,0) direction, and they present a different number of atoms along the (0,0,1) direction. The models are periodic along the (0,1,0) direction, and for all the cases the (1,0,0), (−1,0,0), (0,0,1), and (0,0,−1) surfaces are exposed.

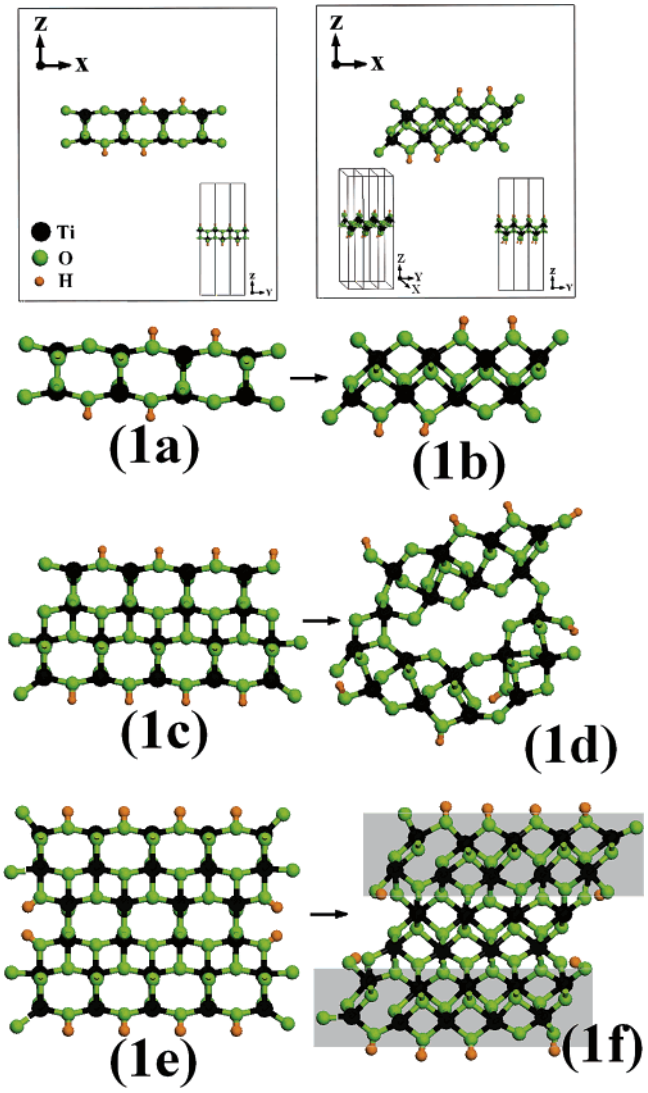

Figure 1. Initial configuration of the anatase wire models used in the calculations: **1a** ($Ti_8O_{18}H_4$), **1c** ($Ti_{18}O_{40}H_8$), and **1e** ($Ti_{28}O_{62}H_{12}$). **1b**, **1d**, and **1f** are final configurations obtained from the ab-MD calculations, where the formation of layers of lepidocrocite-type titanate and the presence of edge-sharing TiO_6 octahedrons are shown. In the box insets above 1a and 1b, the periodic boundary conditions in different directions are shown.

All the models were randomly saturated with hydrogen atoms to ensure the oxidation states under the hypothesis that the titanium has an oxidation state of +4, oxygen of −2, and hydrogen of +1. In this way, the electroneutrality of the whole system is ensured. The hydrogen atoms were placed on the surface of the anatase-type wires, and they play the role of a positive charge. This positive charge could have been introduced as any other positive ion with charge +1, like sodium or potassium, but it is less computationally expensive to model the positive ion with hydrogen. In the experimental hydrothermal alkaline treatment, the positive charge role is played by the Na^+ or K^+ cations. In the following text, we refer to a positive-prototype charge when mentioning the hydrogen atoms.

(32) Fukuda, K.; Nakai, I.; Oishi, C.; Nomura, M.; Harada, M.; Ebina, Y.; Sasaki, T. *J. Phys. Chem. B* **2004**, *108*, 13088.
(33) Armstrong, G.; Armstrong, A. R.; Canales, J.; Bruce, P. G. *Chem. Commun.* **2005**, 2452.
(34) Kolen'ko, Y. V.; Kovnir, K. A.; Gavrilov, A. I.; Farshev, A. V.; Frantti, J.; Lebedev, O. I.; Churagulov, B. R.; Van Tendeloo, G.; Yoshimura, M. *J. Chem. Phys. B* **2006**, *110*, 4030.
(35) Yang, J.; Li, D.; Wang, H. Z.; Wang, X.; Yang, X. J.; Lu, L. D. *Mater. Lett.* **2001**, *50*, 230.
(36) Sugimoto, W.; Terabayashi, O.; Murakami, Y.; Takasu, Y. *J. Mater. Chem.* **2002**, *12*, 3814.
(37) Zhu, H. Y.; Lan, Y.; Gao. X. P.; Ringer, S. P.; Zheng, Z. F.; Song, D. Y.; Zhao, J. C. *J. Am. Chem. Soc.* **2005**, *127*, 6730.
(38) Zhu, H.; Gao, X.; Lan, Y.; Song, D.; Xi, Y.; Zhao, J. *J. Am. Chem. Soc.* **2004**, *126*, 8380.
(39) Yoshida, R.; Suzuki, Y.; Yoshikawa S. *J. Solid State Chem.* **2005**, *178*, 2179.
(40) Morgado, E., Jr.; de Abreu, M. A. S.; Pravia, O. R. C.; Marinkovic, B. A.; Jardim, P. M.; Rizzo, F. C.; Araujo, A. S. *Solid State Sci.* **2006**, *8*, 888.
(41) Chen, Y.-F.; Lee, C.-Y.; Yeng, M.-Y.; Chiu, H.-T. *Mater. Chem. Phys.* **2003**, *81*, 39.
(42) Bavykin, D. V.; Parmon, V. N.; Lapkin, A. A.; Walsh, F. C. *J. Mater. Chem.* **2004**, *14*, 3370.
(43) Morgado, E., Jr.; de Abreu, M. A. S.; Moure, G. T.; Marinkovic, B. A.; Jardim, P. M.; Araujo, A. S. *Chem. Mater.* **2007**, *19*, 665.

Table 1. Some TiO_2 Cell Parameters

phase	cell parameters (Å) a	b	c
anatase[a]	**3.782**	**3.782**	9.502
TiO_2 (B)[b]	12.1787	**3.7412**	6.5249
titanate step 1[c] ($H_2Ti_2O_5 \cdot H_2O$)	19.26	**3.78**	3.0
titanate step 2[b] ($H_2Ti_3O_7$)	16.03	**3.75**	9.19
titanate step 3[d] ($K_2Ti_4O_9$)	18.27	**3.792**	12.04
lepidocrocite titanate[e]	**3.87**	12.51	3.06

[a] Reference 44. [b] Reference 45. [c] Reference 13. [d] Reference 46. [e] Reference 47.

Table 2. *k*-Vector Used in ab-MD Calculations

k-vector			weight
0.00000	0.42857	0.00000	0.285714
0.00000	0.28571	0.00000	0.285714
0.00000	0.14286	0.00000	0.285714
0.00000	0.00000	0.00000	0.142857

It is known that anatase, TiO_2(B), and titanate phases present at least one cell parameter length that is closed to a value of 3.7 Å as shown in Table 1. On the basis of this one-cell parameter similarity, a good first approach, for the simulation of a phase transformation between these phases, is to consider a periodic cell configuration model keeping fixed one of the cell lengths as **b** = 3.7 Å. Because the phase transformation involves expansions and contractions of the atoms array, in our model we establish an empty space region such that the expansions and contractions can take place during the simulation; see box insets above Figure 1a and 1b. The values of the **a** and **c** cell parameters are arbitrarily set to 25 Å and 28.46 Å, respectively. Our calculations consider a constant volume throughout the simulation in an NVT ensemble (i.e., the number of particles N, the volume V, and the temperature T of the system are kept constant).

Thermal effects should be taken into account in the simulation of the phase transformation, and to do this, we choose an ab initio molecular dynamics (ab-MD) procedure in an NVT ensemble. The electronic calculations were carried out using density functional theory (DFT), in particular, we use the non-self-consistent Harris functional,[48] which has extensively been used in ab-MD calculations of semiconducting amorphous materials,[49] and were validated for the case of TiO_2 and titanates by Zhang and co-workers.[19,23] In particular, we use the exchange correlation term of Perdew and Wang[50] together with effective core pseudopotentials[51,52] for the core electrons. We use the minimal basis set as defined in the DMol^3 code[53,54] as instrumented in the interface of Materials Studio.[55] For each case, the DFT calculations were carried out using the Γ-point approximation to facilitate the calculation. Additionally, in section 3.3, the ab-MD calculations were carried out using several *k*-points (see Table 2) in order to consider long-range interactions.

(44) Howard, C. J.; Sabine, T. M.; Dickson, F. *Acta Crystallogr., Sect. B: Struct. Sci.* **1991**, *47*, 462.
(45) Feist, T. P.; Davies, P. K. *J. Solid State Chem.* **1992**, *101*, 275.
(46) Izawa, H.; Kikkawa, S.; Kolzuml, M. *J. Phys. Chem.* **1982**, *86*, 5023.
(47) Ewing, F. J. *J. Chem. Phys.* **1935**, *3*, 429.
(48) Harris, *J. Phys. Rev. B* **1985**, *31*, 1770.
(49) Alvarez, F.; Díaz, C. C.; Valladares, A. A.; Valladares, R. M. *Phys. Rev. B* **2002**, *65*, 113108.
(50) Perdew, J. P.; Wang, Y. *Phys. Rev. B* **1992**, *45*, 13244.
(51) Dolg, M.; Wedig, U.; Stoll, H.; Preuss, H. *J. Chem. Phys.* **1987**, *86*, 866.
(52) Bergner, A.; Dolg, M.; Kuechle, W.; Stoll, H.; Preuss, H. *Mol. Phys.* **1993**, *80*, 1431.
(53) Delley, B. *J. Chem. Phys.* **1990**, *92*, 508.
(54) Delley, B. *J. Chem. Phys.* **2000**, *113*, 7756.
(55) *Accelrys MS Modeling 3.2*; Accelrys, Inc.: San Diego, CA, 2003.

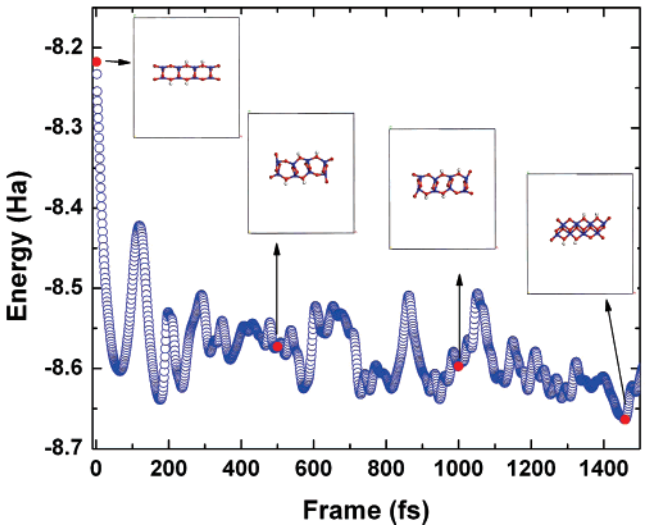

Figure 2. Energy evolution of the anatase wire $Ti_8O_{18}H_4$ **1a** during the ab initio molecular dynamics (ab-MD) transformation to lepidocrocite-type titanate. The insets show the different structural changes that occur during the ab-MD at different times.

The selected thermal process comprises first a lineal melting process from 0 K (−273 °C) to 600 K (327 °C), in 100 steps, and a time step of 1 fs followed by an annealing process at 600 K (327 °C) until the transformation is observed. The melting process is carried out to stabilize the structure before the thermal annealing process. The melting process slowly stabilizes the structure by exposing it to the temperature and by avoiding a drastic introduction of the annealing temperature. The temperature of the annealing process is higher than the experimental temperature used in the hydrothermal treatment of TiO_2 in NaOH to form nanomaterials, which is reported to be in the range of 60−250 °C.[3,10,56,57] Our calculation temperature is chosen higher to accelerate the phase transformation process and to observe it in a reasonable computing time.

Additionally, for the case of the largest wire model, **1e**, we have also performed an ab-MD calculation with the inclusion of an aqueous solution of NaOH to elucidate its effect during the hydrothermal treatment. The number of added water and NaOH molecules is selected to be enough to fill the empty space in the cell. For simplicity of the model and calculation, the ionization of NaOH was not taken into account in the initial configuration. In this case, the available volume, which is the total cell volume minus the volume occupied by the TiO_2 bulk, is equal to 1550 Å^3/unit cell where 9 NaOH and 33 H_2O molecules were included in the initial configuration. In section 3.3, several case studies are presented where different numbers of Na^+OH^- or water molecules are included for the case of models **1a** and **1c**.

3. Results and Discussion

3.1. ab-MD Phase Transformation Analysis. In Figure 2, the energy evolution of the smallest anatase wire $Ti_8O_{18}H_4$ **1a** during the ab-MD calculation is shown. The insets in Figure 2 show the different structural changes that occur during the ab-MD at different times. The cell of the initial configuration contains a periodic atomic array in which the titanium and oxygen atom positions are arranged in an anatase-type structure. The hydrogen atoms (positive-prototype -charges) are bonded to some oxygen atoms to ensure the

(56) Kasuga, T.; Hiramatsu, M. U.S. Patent No. 6,537,517, 2000.
(57) Koyanagi, T.; Shirono, K.; Tanaka, A.; Komatsu, M. U.S. Patent Application No. 2004265587, 2004.

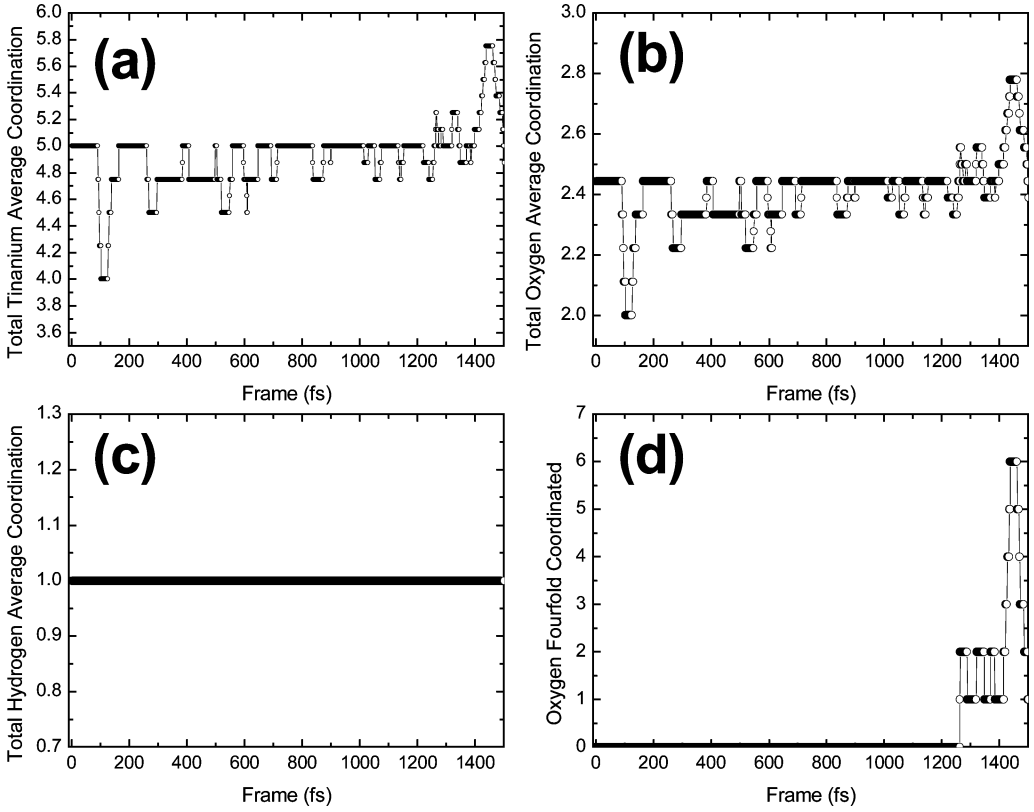

Figure 3. Evolution of the average coordination number (ACN) in the ab-MD during the transformation anatase−lepidocrocite for the model **1a** (Figure 1a). (a) Titanium average coordination number (Ti-ACN), (b) O-ACN, and (c) H-ACN. (d) Number of four-coordinated oxygen atoms.

electroneutrality of the system, and their positions are arbitrary. The size of the wire along the (1,0,0) direction is 15 Å.

In Figure 2, it is observed that the total transformation of the anatase-type wire takes place at around 1455 fs. The final form **1b**, see Figure 1b and the last inset in Figure 2, has a lepidocrocite-type structure, which is a titanate-type structure of infinite step. This final form, **1b**, has a total energy that is lower than the total energy of the original structure by ∼0.44 Ha (∼11.97 eV) thus being energetically more favorable. It could be argued that anatase does not transform into lepidocrocite titanate-type structure at high temperatures, but rather it is reported that it transforms to the rutile phase;[58,59] however, we consider that the anatase-to-lepidocrocite titanate transformation occurs only in the case of no-bulk anatase, that is, no agglomerated or no aggregated small anatase crystals. In Figure 2, two other intermediates of the transformation during the ab-MD calculation are shown, which present deformation of the initial structure into an amorphous configuration that subsequently becomes a lepidocrocite-type structure.

The titanium and oxygen average coordination number, ACN (the number of neighbors surrounding all the Ti or O atoms divided by the total number of Ti or O atoms), in the anatase is different from the ACN in the lepidocrocite structure. Therefore, the ACN value depends on the size of the model, the structure, and the content of atoms. To monitor the transformation anatase−lepidocrocite, we analyzed the change in the ACN property during the ab-MD, and cutoffs of 2.3 Å and 1.28 Å bonding distance for the Ti−O and O−H bonds, respectively, were considered. The Ti-ACN value for the initial **1a** structure is 5.753, and this value shows fluctuations from 4.0 to 5.75 during the transformation as it is shown in Figure 3a. The Ti-ACN of 5.75 corresponds to the final lepidocrocite-type structure **1b**, which is formed at around 1455 fs.

In the initial structure **1a**, there are oxygen atoms with 1, 2, or 3 coordination number; therefore, the initial average coordination number is 2.44. In Figure 3b, it is observed that the initial O-ACN shows fluctuations during the ab-MD toward lower values with a minimum value of 2.00. At around 1255 fs, a change to higher values is observed with a maximum of ∼2.8, which corresponds to the O-ACN in the lepidocrocite-type structure. In the lepidocrocite-type structure **1b**, there are oxygen atoms with coordination numbers of 4, 2, and 1. During the transformation, there is an oxylation process because of the formation of oxygen atoms with coordination 4. The oxylation occurs at around 1255 fs as it is shown in Figure 3d. Thus, the presence of the lepidocrocite-type structure starts at around 1255 fs, and it is completed by 1460 fs. Before 1255 fs, the number of four-coordinated oxygen atoms is zero as it can be seen in Figure 3d. The hydrogen average coordination number remains constant and equal to 1 during the entire process, see Figure 3c.

For each type of atom, the evolution of the total Mulliken charge for the system **1a** is shown in Figure 4. As it can be seen in Figure 4a, the total titanium Mulliken charge shows fluctuations, but in general it shows a decreasing value between the initial configuration and the final lepidocrocite-type structure **1b**. The opposite behavior is observed for the

(58) Depero, L. E.; Bonzi, P.; Zocchi, M.; Casale, C.; De Michele, G. *J. Mater. Res.* **1993**, *8*, 2709.
(59) Yu, X.-F.; Wu, N.-Z.; Xie, Y.-C.; Tang, Y.-Q. *J. Mater. Sci. Lett.* **2001**, *20*, 319.

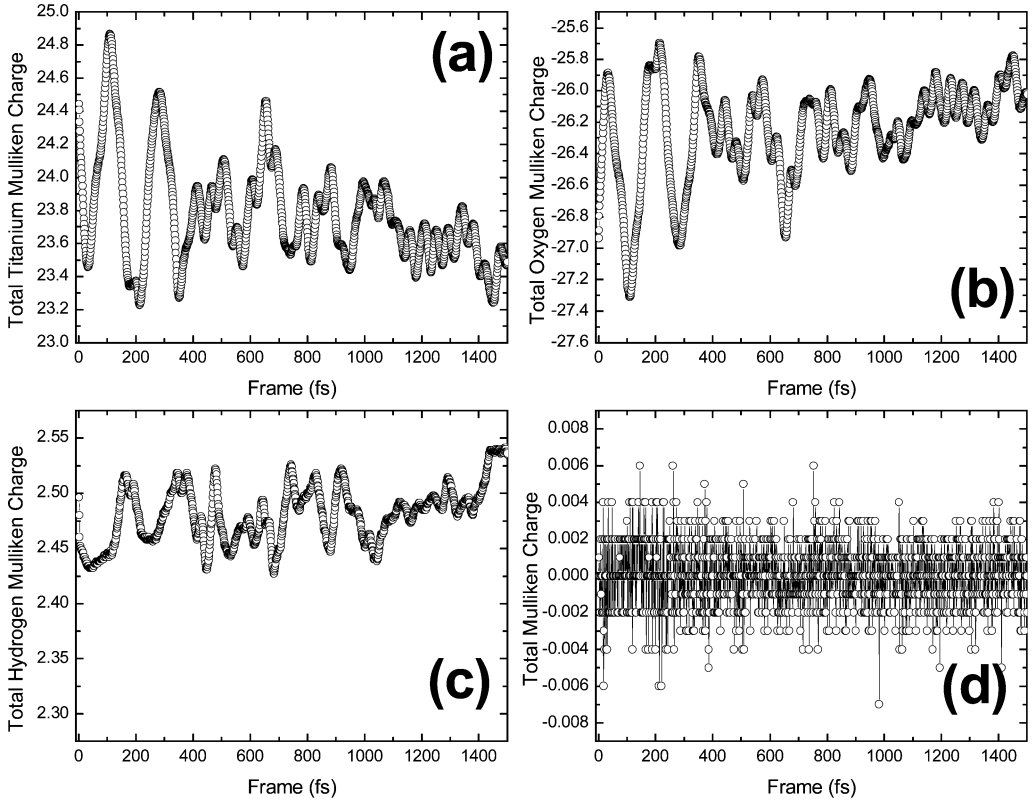

Figure 4. Total Mulliken charge evolution for (a) titanium, (b) oxygen, (c) hydrogen, and (d) total system.

oxygen atoms where an increase in the total Mulliken charge is found, see Figure 4b. No important change is observed in the Mulliken charge for the case of the hydrogen atoms, see Figure 4c. Therefore, it can be concluded that there is only charge transfer between the Ti and O atoms during the phase transformation. By looking at Figure 4a and 4b, it can be said that the charge transfer goes from the oxygen atoms (donors) to the titanium atoms (acceptors) because the total titanium Mulliken charge, in the final configuration, is less positive than in the initial configuration, and the total oxygen Mulliken charge is less negative in the final configuration. This agrees with an increase of the oxygen coordination number to 4, during the formation of the lepidocrocite-type titanate, because some oxygen atoms form a coordination bond with titanium. The electroneutrality of the system is kept during the transformation with very small fluctuations as it can be seen in Figure 4d.

To analyze the size effect on the transformation, we carried out the ab-MD calculation using a bigger anatase-type system. For this calculation, we use the model **1c** with the formula $Ti_{18}O_{40}H_8$ (see Figure 1), and we found that the transformation takes place too as in the former system **1b**; however, some differences are found. In the final structure **1d** (see Figure 1), two layerlike regions are formed, which are bonded just at the ends. It looks like these two layers might separate, which can be considered as the first step of the exfoliation process that has been proposed to occur during the hydrothermal treatment, in the synthesis of TiO_2 nanotubes, to form a layered product from a raw anatase phase.[8]

In Figure 5, it is observed that the total transformation to lepidocrocite-type structure **1d** occurs at around 3480 fs. The final lepidocrocite-type structure **1d** is constituted by two

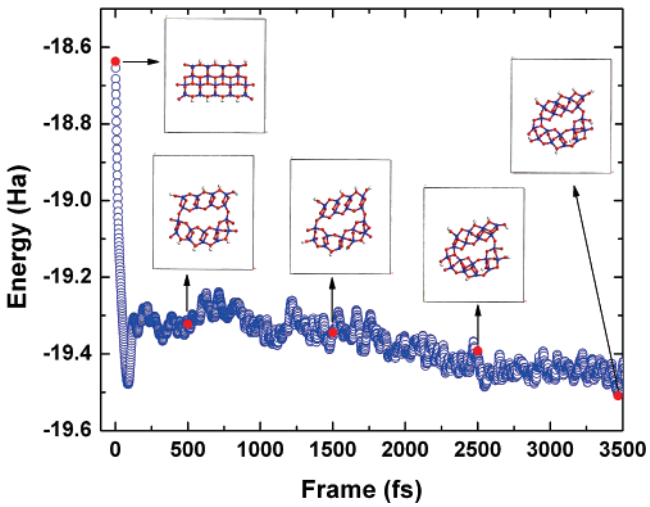

Figure 5. Energy evolution of the anatase wire $Ti_{18}O_{40}H_8$ model **1c** during the transformation to two laminar lepidocrocyte-type titanate **1d**. The insets show the different structural changes that occur during the ab-MD at different times.

lepidocrocite-type layers bonded at the ends, and it has a total energy that is lower than the total energy of the original structure **1c** by ~0.87 Ha (~23.67 eV). Thus, the final lepidocrocite-type structure **1d** is energetically more favorable than the anatase-type structure as in the former case. Therefore, we consider that the size of the initial structure plays a major role in the product of the transformation. For all the atoms, the atom average coordination number shows fluctuations during the ab-MD. In Figure 6, the corresponding graphics are shown. For the case of the titanium and oxygen atoms, it is observed, in general, an ascendant behavior in their average coordination numbers, see Figure 6a and 6b. For the case of the hydrogen atom, there are small fluctua-

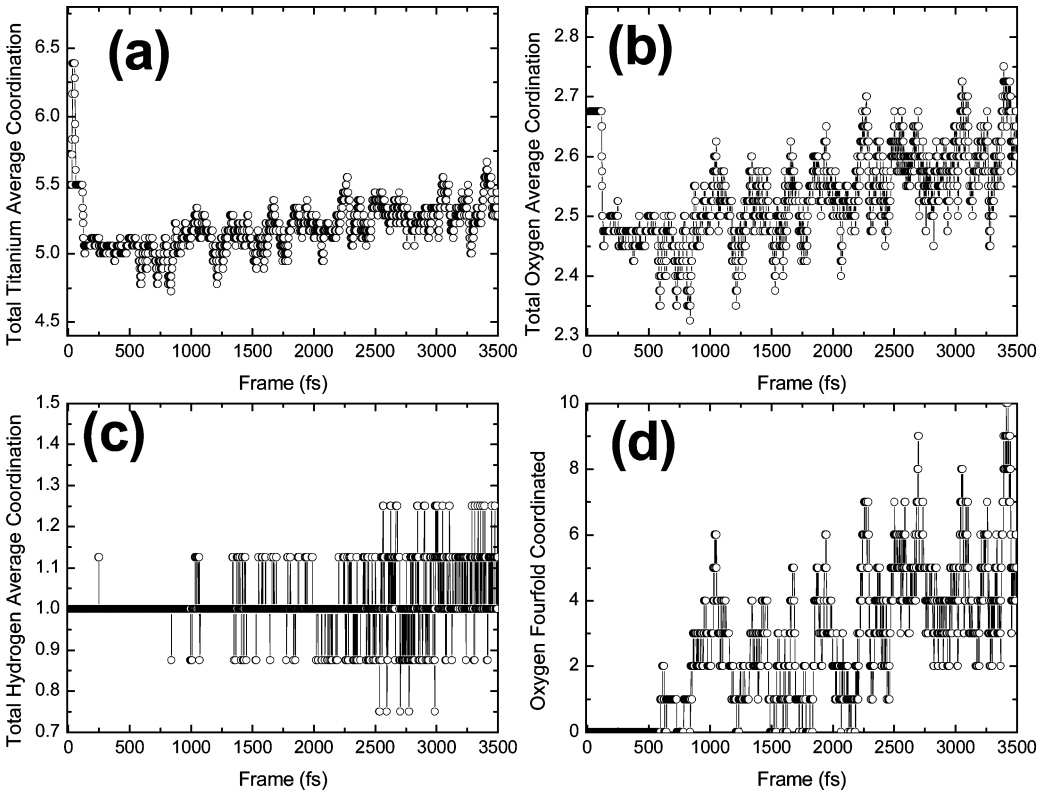

Figure 6. Evolution of the average coordination number (ACN) in the ab-MD during the transformation anatase−lepidocrocite for the model **1c** (Figure 1c). (a) Titanium average coordination number (Ti-ACN), (b) O-ACN, and (c) H-ACN. (d) Number of four-coordinated oxygen atoms

tions but in general the average coordination number is equal to 1, see Figure 6c.

The beginning of the anatase−lepidocrocite phase transformation is monitored by the formation of oxygen atoms with a coordination of 4. In the anatase, the four-coordinated oxygen atoms are not present. For this case, we observe the presence of four-coordinated oxygen atoms at around 590 fs, see Figure 6d. The number of four-coordinated oxygen atoms tends to increase during the ab-MD reaching the highest value of 10, see Figure 6d.

The analysis of the Mulliken charge for the anatase−lepidocrocite phase transformation for the **1c** system is shown in Figure 7. As in the former case, a charge transfer is observed that goes from oxygen to titanium atoms, see Figure 7a and 7b. Because this system is bigger than the former, the fluctuations in the Mulliken charge are smaller, see Figures 7a, 7b, 4a, and 4b. It is observed that the hydrogen atoms have a decrease of their average Mulliken charge, Figure 7c, and this means that there are oxygen atoms transferring charge to hydrogen atoms. In **1d**, it is observed that there are hydrogen atoms too close to oxygen atoms, right at the junction of the layers, and these oxygen atoms might be transferring charge to these closest hydrogen atoms. The electroneutrality of the system is kept during the entire transformation as it is shown is Figure 7d.

In Figure 8, the ab-MD energy evolution of the largest calculated anatase-type wire model ($Ti_{28}O_{62}H_{12}$ **1e**) is shown. The formation of the final configuration ends at around 3500 fs. Again, the final configuration (**1f** in Figure 1) is energetically more favorable than the initial configuration as in the former cases. The final configuration (see last inset in Figure 8 and **1f** in Figure 1) shows the presence of three different regions that correspond to laminar lepidocrocite-type titanate with the characteristic edge-sharing TiO_6 octahedrons. However, these layers are still bonded together. In Figure 1f, the different regions are highlighted. In Figure 10g, a side view is shown of the product **1f** where it can be seen that there is a shift of the intermediate layer with respect to the external layers. It could be expected that because of thermal effects these layers might separate but to observe this phenomena would require a longer simulation time. Looking at the sequence of insets in Figure 8, it can be said that the transformation to the lepidocrocite-type titanate takes place first in the outer layers and finally the transformation takes place in the middle layer. The transformation seems to be sequential, as shown in the insets, starting in one region and growing as a seed to the other regions.

As in the former cases, during the transformation of the largest anatase-type wire model ($Ti_{28}O_{62}H_{12}$ **1e**), an increase in the titanium and oxygen average coordination numbers is observed, while the hydrogen ACN shows some fluctuations around 1. For this case, the formation of the tetracoordinated oxygen atoms is found to begin at around 600 fs. In Figure 8, third inset, which corresponds to a time beyond 600 fs, it is observed that in the lower region of the model there is formation of tetrahedral oxygen atoms. Also, as in the former cases, there is a donation of charge from the oxygen atoms to the titanium atoms and in some cases, as in the transformation of **1c** to **1d**, there are oxygen atoms at the end of the outer regions that seem to donate electron density to the closest hydrogen atoms (positive-prototype charges), but the system remains neutral during the entire process.

To elucidate the effect of the NaOH during the hydrothermal treatment of anatase, we have also performed an ab-

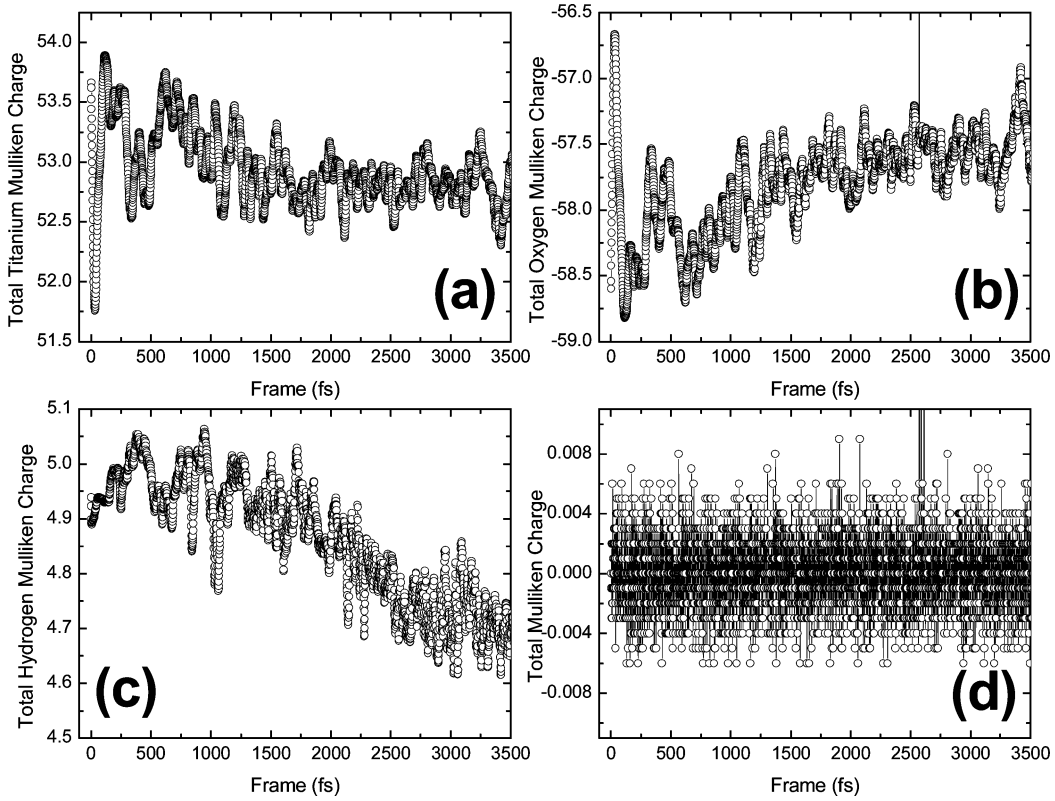

Figure 7. Total Mulliken charge evolution for (a) titanium, (b) oxygen, (c) hydrogen, and (d) total system.

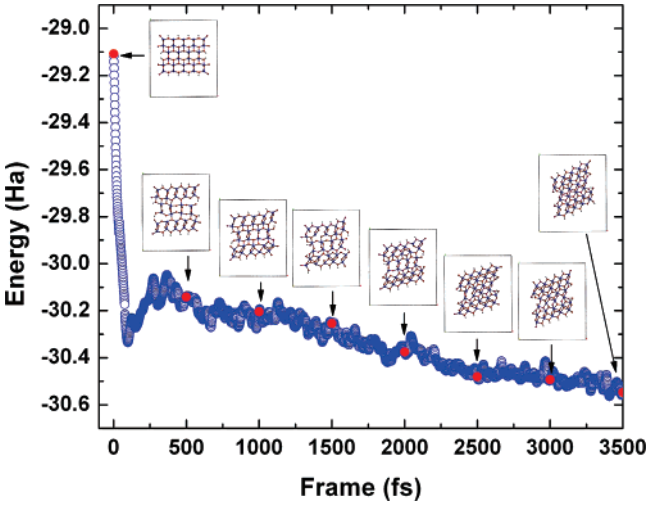

Figure 8. Energy evolution of the anatase wire model $Ti_{28}O_{62}H_{12}$ **1e** during the transformation to a quasilayer lepidocrocyte-type titanate **1f**. The insets show the different structural changes that occur during the ab-MD at different times.

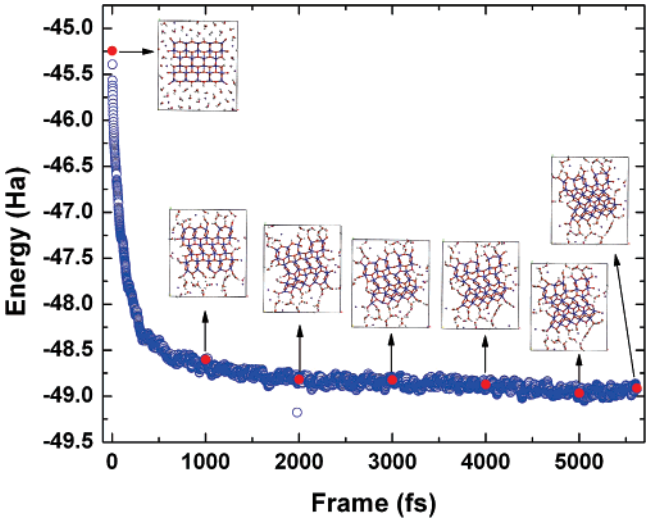

Figure 9. Energy evolution of the largest anatase wire model $Ti_{28}O_{62}H_{12}$ **1e** with the inclusion of NaOH and H_2O during the transformation to a quasilayer lepidocrocyte-type titanate. The insets show the different structural changes that occur during the ab-MD at different times.

MD calculation with the inclusion of NaOH and H_2O for the case of the largest anatase-type wire model ($Ti_{28}O_{62}H_{12}$ **1e**). The number of added water and NaOH molecules is selected to be enough to fill the empty space in the cell. For simplicity of the model and calculation, the ionization of NaOH was not taken into account in the initial configuration. We included 9 NaOH molecules and 33 H_2O molecules in the initial configuration. The initial configuration was obtained from geometry optimization of the surrounding entities (NaOH and H_2O) keeping fixed the coordinates of the anatase-type structure. The geometry optimization was done by performing forcefield-based minimization using the energy minimization panel in Cerius2 version 4.6 and the COMPASS (Condensed-Phase Optimized Molecular Potentials for Atomistic Simulation Studies)[60,61] consistent force field as it is provided in the Cerius2 package.[62]

In Figure 9, the energy evolution during the ab-MD calculation is shown. Because of the presence of the NaOH and H_2O molecules, the energy fluctuations are smaller. By looking at the inset sequence in Figure 9, it can be seen that

(60) Sun, H.; Ren, P.; Fried, J. R. *Comput. Theor. Polym. Sci.* **1998**, *8*, 229.
(61) Sun, H. *J. Phys. Chem. B* **1998**, *102*, 7338.
(62) *Cerius2 Modeling Environment*, release 4.0; Molecular Simulations Incorporated: San Diego, CA, 1999.

the transformation also takes place in a sequential way but in a less orderly fashion because of the interaction of the anatase-type wire with the surrounding molecules. The final structure, see last inset in Figure 9, shows that the transformation to the characteristic TiO_6 octahedrons of titanate-type structure took place only in one outer region and in the central region already discussed in the case of the **1f** product. The top layer shows an amorphous structure due to the interaction with the surrounding molecules. However, this final structure is energetically more favorable than the initial one. For this particular simulation, it is observed that the presence of NaOH and H_2O molecules inserts chaos in the process because of the presence of many degrees of freedom in the system. In this simulation, the effect of NaOH is not evident because the oxygen atoms in the (0,0,1) and (0,0,−1) surfaces are saturated with the prototype-positive charge (hydrogens) in the initial configuration, which inhibits the interaction of the surface with the surrounding NaOH molecules. Therefore, when comparing the process of the transformation in Figures 8 and 9 (with and without NaOH), no appreciable effect is observed. In section 3.3, the effect of NaOH is analyzed in more detail.

3.2. Phase Transformation Mechanism. In Figure 10, the steps of the transformation mechanism of anatase to lepidocrocite are presented. In the initial stage, Figure 10a and Figure 10b, the internal oxygen atomic layers (region 1 and region 2) are shifted as the arrows show. This shifting produces the structure shown in Figure 10c. Furthermore, during the shifting process, the oxygen atoms, marked by the arrows in region 2, are twisted or rotated creating an angle between them as it is shown in Figure 10c. The effect of the shifting−twisting process is to leave the involved oxygen atoms too close to titanium atoms to form new Ti−O bonds, see arrows in Figure 10c. Because of the new Ti−O bond formation, the original three-coordinated oxygen atoms in anatase become tetracoordinated, and this is why the transformation anatase−lepidocrocite is monitored by the formation of tetracoordinated (T_h) oxygen atoms. The formation of the T_h oxygen atoms forces a distortion of the different layers as shown in Figure 10d. The distortion can be appreciated by comparing Figure 10d with Figure 10c.

Figure 10e is the same as Figure 10d where some of the internal Ti−O bonds were deleted to highlight that, at this stage, there is the formation of lepidocrocite-type layers, which are still joined forming a lepidocrocite bulk or a three-dimensional lepidocrocite array. Simultaneously to the formation of the lepidocrocite-bonded layers, the middle layer becomes dislocated with respect to the external layers. In Figure 10f and Figure 10g, a lateral view of the initial anatase structure and the final lepidocrocite-type bulk are shown, where the dislocation of the internal layer can be observed. We could say that if the dislocation is too large then the bonds would break forming the lepidocrocite-type layers shown in Figure 10e. We found that all the discussed stages in Figure 10 take place in a sequential way, and they take place initially in a small portion of the crystal and then propagate to the entire structure.

The layers shown in Figure 10e are the construction unit in the formation of any layered titanate and of TiO_2 (B)

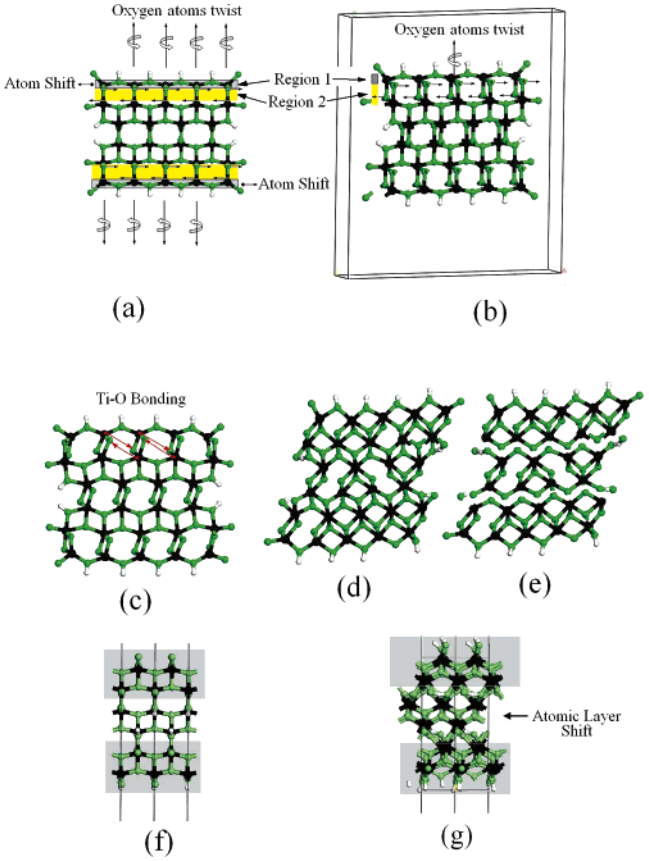

Figure 10. Schematic representation of the different stages in the mechanism of the anatase- to lepidocrocite-type titanate phase transformation. (a) and (b) are initial configurations, where the initial atomic shifts and oxygen atom twisting are indicated. (b) This is a slightly rotated view of crystal shown in (a). (c) This figure shows the structure shifted and twisted where the formation of tetracoordinated (T_h) oxygen atoms is indicated. (d) After formation of the T_h oxygen atoms, the crystal structure is distorted as shown here. (e) This figure is the same one shown in (d) but where we have deleted the internal bonds to show that lepidocrocite-type titanate layers are clearly formed. (f) and (g) are side views of the initial anatase structure and the final lepidocrocite structure, respectively. In (g), the internal layer dislocation can be observed.

phase. The titanates and the lepidocrocite-type titanate as well as TiO_2 (B) have a common region in their structure. This common region is composed of edge-sharing TiO_6 octahedrons, shown in Figure 10e. The lepidocrocite-type titanate is formed by layers of an infinite sequence of the edge-sharing TiO_6 octahedrons while the titanates are formed by a finite sequence of the edge-sharing TiO_6 octahedrons, which are joined at the corners to form a "stepped" layered structure. In Figure 11, the following structures are shown: step 1 to step 5 titanates (Figure 11a− Figure 11e, respectively), lepidocrocite-type titanate, which shows infinite edge-sharing TiO_6 octahedrons layers (Figure 11f), and TiO_2 (B) phase. The TiO_2 (B) phase is composed of corrugated sheets of edge- and corner-sharing TiO_6 octahedrons, but the sheets are joined together to form a three-dimensional framework (Figure 11g).

Depending on the experimental conditions, that is, time of reaction, temperature, and NaOH concentration, during the hydrothermal treatment of anatase with NaOH, the formation of layered titanates with different step, lepidocrocite, and TiO_2 (B) is possible as we showed in the mechanism presented in Figure 10. In the formation of the layered step titanates, the presence of defects in the structure shown in

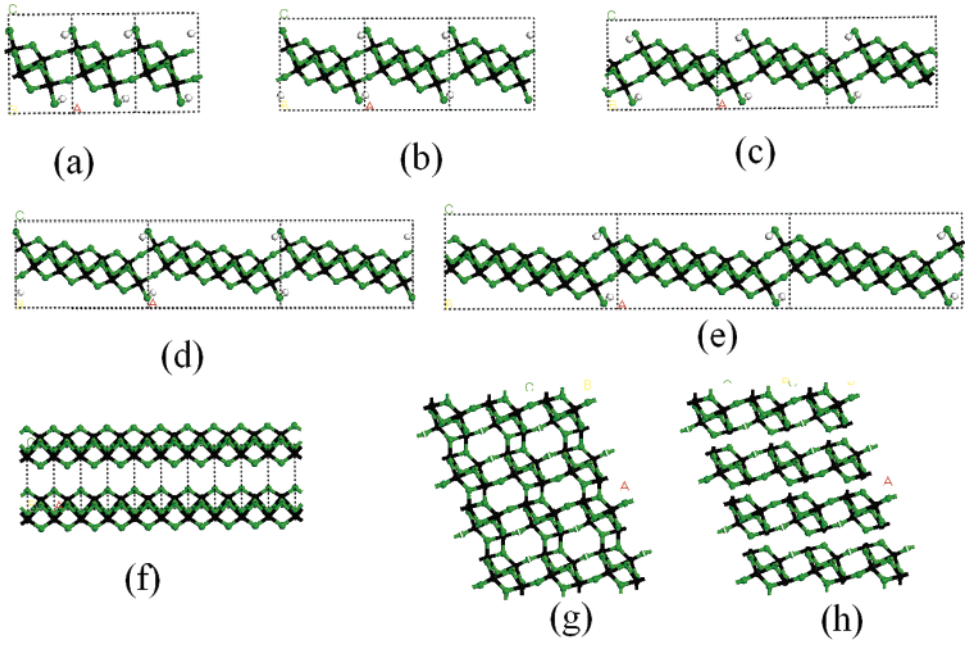

Figure 11. (a−e) Structure of titanates step 1 to step 5, respectively. (f) structure of lepidocrocite, which is a titanate of infinite step (step ∞). (g) Structure of TiO_2 (B). (h) This structure is the same presented in 11g where we have deleted some internal bonds to show that the bulk TiO_2 (B) phase is composed of layers of titanate step 1 (see 11a).

Figure 10e determines the type of formed titanate, which can be step 1, step 2, step 3, and so forth; see Figure 11a−11e. As said before, the titanates are formed by a finite sequence of the edge-sharing TiO_6 octahedrons, which are joined at the corners to form a "stepped" layered structure. We use the term "defect" to define the "step" between two finite lepidocrocite layers to form a titanate of finite step. As mentioned in the Introduction, the following step titanate structures have been proposed to be the unit cell in the TiO_2 nanostructures: $H_2Ti_2O_5 \cdot H_2O$,[13,14] $H_2Ti_3O_7$,[15−23] and $H_2Ti_4O_9 \cdot H_2O$,[24] which correspond to titanates of step 1, step 2, and step 3, respectively (see Figure 11a, 11b, and 11c).

In the formation of lepidocrocite, which is a titanate of infinite step, there is no presence of defects in the union of the titanate layers shown in Figure 10e forming in this way the perfect lepidocrocite-layered structure (see Figure 11f). Fukuda et al.[32] and Ma et al.[26] have mentioned that lepidocrocite is the construction unit in the TiO_2 nanostructures obtained from the hydrothermal treatment of anatase with NaOH.

In the formation of TiO_2 (B), Feist and Davies reported that proton exchange and subsequent dehydration of layered titanates yield TiO_2 (B) at temperatures below 350 °C.[40] Consequently, we consider that TiO_2 (B) can be formed in a sequence that first includes the formation of a titanate of step 1 ($H_2Ti_2O_5 \cdot H_2O$), following the mechanism discussed in Figure 10. Second, a proton exchange and dehydration of the step 1 titanate forms TiO_2 (B). In Figure 11g, the structure of TiO_2 (B) is presented. The structure in Figure 11h is the same as presented in Figure 11g where we have deleted some internal bonds to show that the bulk TiO_2 (B) is composed of layers of the step 1 titanate (see Figure 11a). Armstrong et al.[33] have proposed that TiO_2 (B) is the building block of the TiO_2 nanostructures formed in the hydrothermal treatment.

Finally, it is reported that anatase is the building block in the TiO_2 nanostructures obtained from the hydrothermal treatment of anatase with NaOH.[3−10,12] In this particular case, the inverse mechanism has to be considered (titanate to anatase). In the literature, there are presented hypothetical schemes, which are obtained from experimental observations, where the inverse path (titanate to anatase) is considered,[37,39,40,63] and on the basis of the observation of the products, it is reported that the inverse path involves titanate to TiO_2 (B) to anatase.[39,40]

We consider that our mechanism, presented in Figure 10, helps to understand, at atomic level, the formation of anatase from lepidocrocite-type titanate, through the inverse mechanism. First, layered titanate has to be formed, as explained above. Second, several stacked and dislocated layers of titanate, shown in Figure 10e, are pushed together and bonded to form the structure shown in Figure 10d and in Figure 10g, which is a bulk titanate. Then, the inverse process shown in Figure 10, 10c to 10b and 10a, takes place to produce anatase. Experimentally, this inverse transformation process can be reached either from acid wash or calcination (at around 600 °C) of the as-formed titanate.[37,39,40,63]

3.3. Different Surface Environments and Inclusion of Several *k*-Points in the ab-MD Calculations. As mentioned in the Computational Details section, the former calculations were carried out using the Γ-point approximation. In this section, we investigate the effect on the transformation because of the inclusion of several *k*-points in the ab-MD calculations. The cell dimension along the **b** direction in the used models (Figure 1) is narrow; thus, to check the long-range periodicity effects, we include several *k*-points in our calculations. In Table 2, the *k*-vectors used are shown. All the following results were obtained carrying out calculations using several *k*-points. For those cases where water or Na^+OH^-molecules are surrounding the anatase-type model, the initial configuration was obtained from geometry opti-

(63) Nian, J.-N.; Teng, H. *J. Phys. Chem. B* **2006**, *110*, 4193.

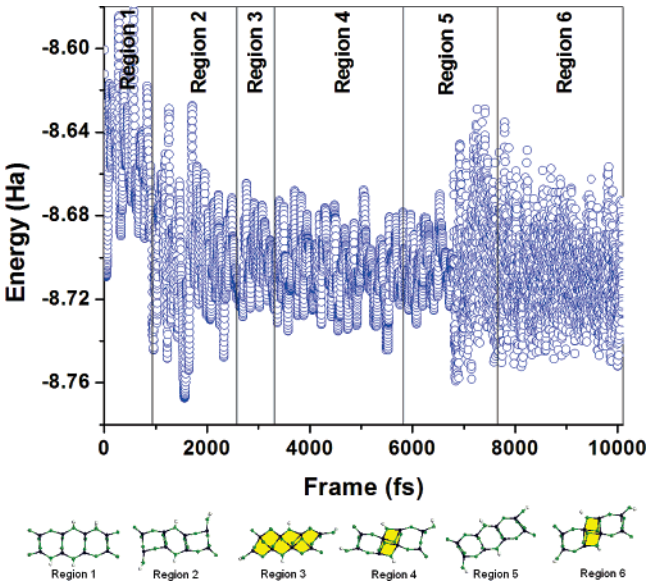

Figure 12. Energy evolution of the anatase wire $Ti_8O_{18}H_4$ **1a** during an ab initio molecular dynamics (ab-MD) transformation that includes several *k*-points. The structures below the graphic show the different structural changes that occur during the ab-MD at different times and in different regions.

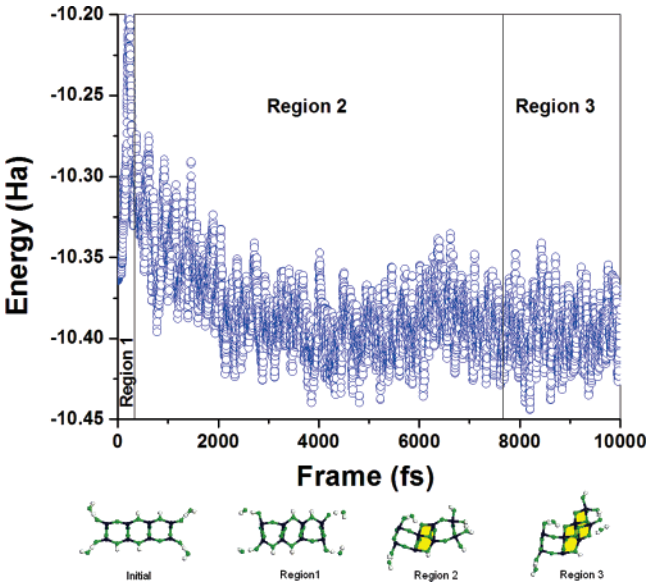

Figure 13. Energy evolution of the anatase wire $Ti_8O_{18}H_4$ (**1a**) + $4H_20$ molecules, which form hydrogen bonds with the oxygen atoms at the external ends. The ab initio molecular dynamics (ab-MD) transformation includes several *k*-points. The structures below the graphic show the different structural changes that occur during the ab-MD at different times and in different regions.

mization of the surrounding entities (Na^+OH^- or H_2O) keeping fixed the coordinates of the anatase-type structure. The geometry optimization was carried out using the same DFT computational methodology as in the MD calculations, and it was stopped in 100 geometry optimization steps to reduce the stress of the initial structure.

*3.3.1. Effect of the Inclusion of Several k-Points for System **1a**.* In Figure 12, the energy evolution of the anatase-type wire $Ti_8O_{18}H_4$ **1a** is shown. This calculation is similar to the one presented in Figure 2 but with the inclusion of several *k*-points (Table 2). As it can be seen in Figure 12, the evolution of the energy presents an oscillatory behavior compared with the one observed in Figure 2. We have divided the energy evolution graph into several regions, which are characterized by small structural fluctuations of the structures presented below the graphic (see Figure 12). We observe that the initial anatase-type configuration (region 1) is transformed to a lepidocrocite-type structure (region 3), at around 2600 fs, by following the same mechanism shown in Figure 10. There is an intermediate step (region 2) where there is a displacement of hydrogen atoms (positive-prototype charge, see Computational Details) to the external oxygen atoms. The transformation to the lepidocrocite-type structure in Figure 12 is slower than the transformation shown in Figure 2, and this is due to the inclusion of several *k*-points in the calculation.

In the sequence of region 4 to region 6 (Figure 12), an inverse transformation can be observed going from lepidocrocite-type to anatase-type structure and vice versa. During this back and forth transformation, because of thermal effects, only the middle section in the structure is transformed, as it is shown in the highlighted middle section in the structures corresponding to region 4 to region 6 (see Figure 12).

*3.3.2. Effect of Saturating the External Oxygen Atoms in System **1a**.* In the ab-MD calculation of system **1a** shown in Figure 2, the external oxygen atoms were monocoordinated, and it can be considered that these oxygen atoms might be unstable and that this oxygen coordination could affect the transformation. Therefore, water has been introduced in the calculation which forms hydrogen bonds with the external oxygen atoms; see the initial configuration structure in Figure 13. In Figure 13, the energy evolution, considering also several *k*-points (Table 2), is shown. It can be seen that there are several transformation regions. Essentially, in region 1, there are structural fluctuations of the anatase-type structure. In region 2, it is observed that in the middle section of the anatase-type structure there is a transformation to lepidocrocite-type structure, and an extension of the transformed section is observed in region 3. Thus, the monocoordination of the oxygen atoms at the ends of the wire versus bicoordination does not seem to be a determinant factor for the transformation to occur, and we find that the transformation follows the same mechanism proposed in Figure 10, but it occurs in a slower manner and with more fluctuations because of the presence of more degrees of freedom.

*3.3.3. Effect of H_2O Presence in the ab-MD of System **1a**.* Another case of the effect of external oxygen saturation is shown in Figure 14, where there are hydrogen atoms only at the edges of the anatase-type structure, which are compensating the charge electroneutrality as a positive-prototype charge (see Computational Details). To study the effect of the presence of water molecules in the transformation, the model was surrounded by six water molecules. The initial configuration was obtained from a geometry optimization, keeping fixed the coordinates of **1a** and optimizing the H_2O positions. In the optimized initial structure, the hydrogen from water is interacting with the $(0,0,\pm1)$ surfaces and acts also as the positive-prototype charge, see initial structure in Figure 14. For this case, we found two main regions as it can be seen in Figure 14. Region 1 is characterized by thermal structural fluctuations of the initial anatase-type

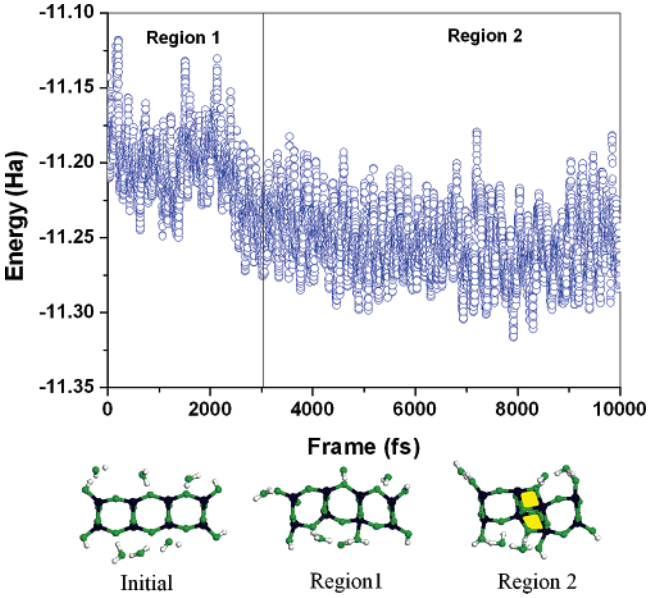

Figure 14. Energy evolution of the anatase wire $Ti_8O_{18}H_4$ (**1a**) + $6H_20$ molecules. For this system, there are hydrogen atoms only at the edges of the anatase-type structure which is surrounded by six water molecules. The ab initio molecular dynamics (ab-MD) transformation includes several *k*-points. The structures below the graphic show the different structural changes that occur during the ab-MD at different times and in different regions.

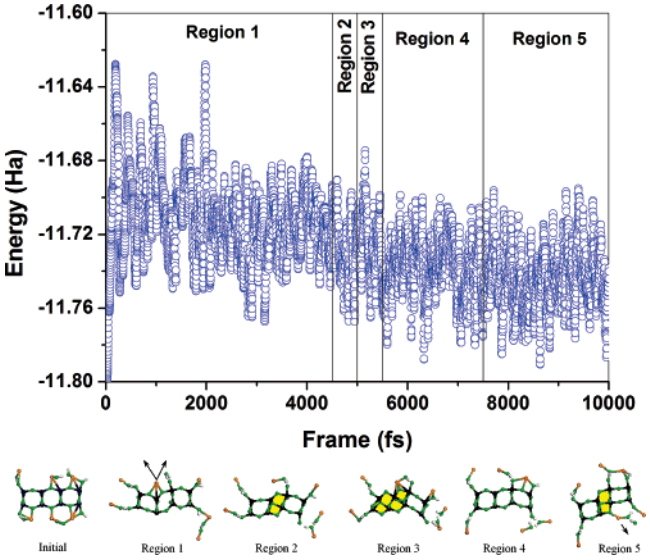

Figure 15. Energy evolution of the anatase wire $Ti_8O_{18}H_4$ (**1a**) in which there are hydrogen atoms only at the edges of the anatase-type structure, including the presence of six NaOH molecules. The initial configuration was obtained from a geometry optimization of the Na^+OH^- entities keeping fixed the coordinates of the anatase-type structure. The ab initio molecular dynamics (ab-MD) transformation includes several *k*-points. The structures below the graphic show the different structural changes that occur during the ab-MD at different times and in different regions.

structure (see structures in Figure 14), followed by region 2 in which the middle section of the anatase-type structure is transformed into the characteristic edge-sharing TiO_6 octahedron of lepidocrocite-type titanate. At the middle section of the compound, where the transformation takes place, the presence of positive charges is observed on the surface (represented, in this case, by the hydronium ion and hydrogen from water molecules); therefore, it could be said that the presence of positive charges on the (0,0,±1) surfaces promotes the transformation. If the six water molecules are not included in the calculation and if there are no positive-prototype charges on the (0,0,±1) surfaces of the anatase-type structure, the transformation does not take place and only structural fluctuations of the anatase-type wire are observed. Consequently, it can be considered that the presence of positive charges interacting with the external oxygen atoms, on the (0,0,±1) surfaces, seems to promote the transformation.

*3.3.4. Effect of NaOH Presence in the ab-MD of System **1a**.* To try to understand the effect of the presence of NaOH in the transformation, a calculation of system **1a** was carried out including the saturation of the monocoordinated oxygen atoms, located at the edges, with hydrogen (positive-prototype charge), and including the presence of six Na^+OH^- molecules. The initial configuration was obtained from a geometry optimization, keeping fixed the coordinates of **1a** and optimizing the Na^+OH^- positions. In the optimized initial structure, the Na^+ is interacting with the (0,0,±1) surfaces and acts as the positive-prototype charge, see initial structure in Figure 15. In the initial configuration as well as in all the other structures shown in Figure 15, the sodium atomic bond is explicitly shown to understand its role in the transformation. Region 1 is dominated by the thermal fluctuations of the anatase-type structure, but at the end of this region, the formation of a three-coordinated Na^+ is observed which is bonded to two oxygen atoms and one titanium atom. This sodium bonding stresses the (0,0,1) surface, produces a deformation of the anatase-type structure, and promotes the formation of the characteristic edge-sharing TiO_6 octahedron (see region 2 in Figure 15) by following the proposed mechanism in Figure 10. Again, the presence of positive-prototype charges (in this case, sodium) interacting with the (0,0,±1) surfaces of the anatase wire promotes the transformation.

Because of the thermal fluctuations of the system, a second edge-sharing TiO_6 octahedron is formed in region 3. Furthermore, also because of the thermal fluctuations, all the edge-sharing TiO_6 octahedrons are transformed into anatase-type structure in region 4. Finally, in region 5, it is observed that a lepidocrocite-type titanate section is formed at the middle part of the compound and that a Na^+OH^- molecule is bonded to the surface right on this section.

*3.3.5. Effect of Saturating the External Oxygen Atoms in System **1c**.* To analyze the size effect on the transformation with the inclusion of several *k*-points and the effect of the saturation of the external oxygen atoms, we carried out the ab-MD calculation using model **1c**, where all the formerly monocoordinated external oxygen atoms have been saturated with positive-prototype charges (in this case simulated by hydrogen). Since in the former calculations, described in this section, we observe that the presence of prototype-positive charges on the (0,0,±1) surfaces is a determining factor for the transformation to take place, and to reduce the complexity in the following calculation, we have only included two prototype-positive charges on the (0,0,±1) surfaces of the initial structure.

In Figure 16, the energy evolution during the ab-MD calculation is shown. The configuration of the initial structure is presented below the graph. In this case, we observe only three predominant regions. In Region 1, we observe a deformation of the anatase-type structure. In region 2, the

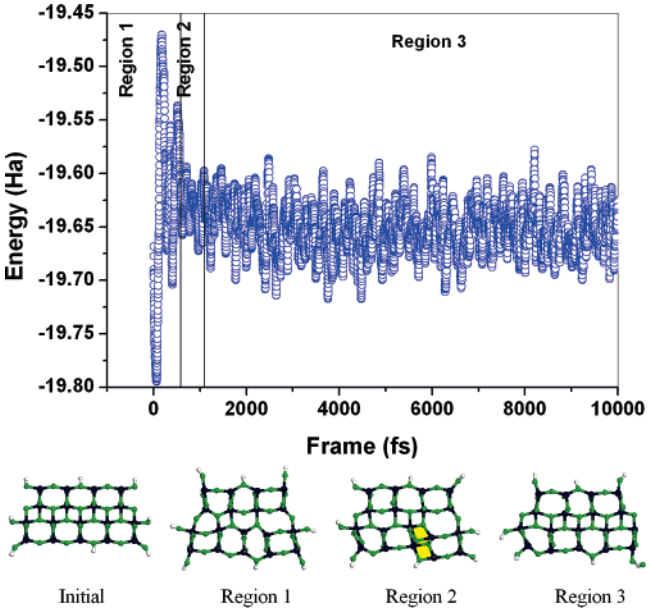

Figure 16. Energy evolution of the anatase wire $Ti_{18}O_{40}H_8$ (**1c**) in which a rearrangement of the hydrogen atoms has been performed to have hydrogen atoms bonded to the oxygen atoms at the ends of the structure. Thus, the hydrogen density on the plane (0,0,1) has been reduced compared with the simulation carried out in Figure 5. The ab initio molecular dynamics (ab-MD) transformation includes several *k*-points. The structures below the graphic show the different structural changes that occur during the ab-MD at different times and in different regions.

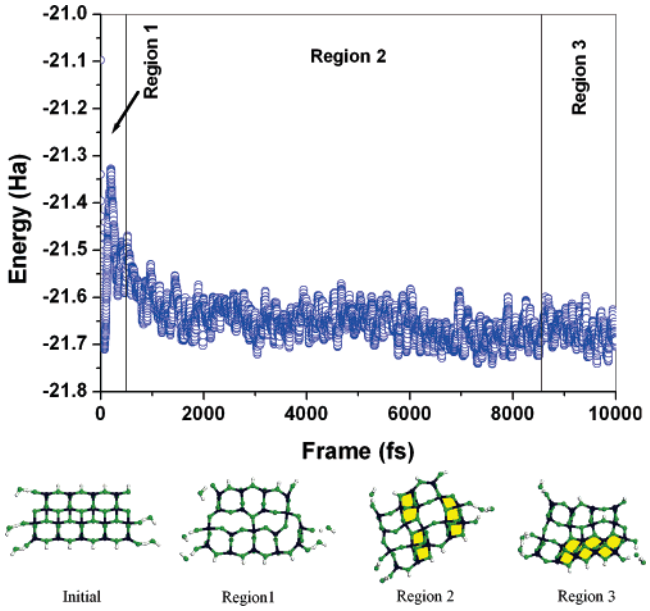

Figure 17. Energy evolution of the anatase wire $Ti_{18}O_{40}H_8$ (**1c**) + $5H_20$ molecules. The water molecules are forming hydrogen bonds with the external oxygen atoms which are at the ends of the structure. The ab initio molecular dynamics (ab-MD) transformation includes several *k*-points. The structures below the graphic show the different structural changes that occur during the ab-MD at different times and in different regions.

formation of an edge-sharing TiO_6 octahedron is observed in a small portion of the compound because of the presence of the positive-prototype charges on the (0,0,±1) surfaces of that section. Because of the thermal fluctuations, it is observed that in region 3 the edge-sharing TiO_6 octahedron is transformed back to anatase-type section.

In Figure 17, we have carried out the calculation of system **1c** with the inclusion of several *k*-points, the saturation of the external oxygen atoms with water molecules, and the saturation of the entire (0,0,±1) surfaces with positive-prototype charges represented by hydrogen. The structure of the initial configuration is shown in Figure 17. For this case, we observe three predominant regions in the ab-MD evolution. The first region is mainly characterized by fluctuations of the anatase-type structure. In region 2, the formation of TiO_2 (B) type structure is observed, which is formed following the same mechanism proposed and discussed in Figures 10 and 11. Finally, in region 3, it is observed that an important section of the compound is transformed to a sequence of three TiO_6 edge-sharing octahedrons by the conversion of the titanate step 1 (TiO_2 (B) type) to a titanate step 3. By comparing with the energy evolution and analysis presented in Figure 16, we could say that the formation of the titanate section in Figure 17 is promoted by the presence of a high density of positive charges on the surface of the initial structure.

*3.3.6. Effect of NaOH Presence in the ab-MD of System **1c**.* For this case, we carried out the same type of calculation described in section 3.3.4 but using **1c** as the anatase model. After 10 000 fs MD steps, no transformation was observed. When only the Γ-point is included in the calculation, the transformation to lepidocrocite-type titanate structure is observed within 1000 fs. Therefore, the inclusion of several *k*-points considerably slows the simulation of the transformation, and it could occur beyond 10 000 fs. When we perform this same calculation but only considering the Γ-point approximation with inclusion of a Na^+ environment, we observe that again the Na^+ interacts with the surface of the anatase-type wire deforming the net and allowing the shift and twist mechanism, explained in Figure 10.

4. Conclusions

In this theoretical work, the mechanism, at atomic level, for the phase transformation of anatase- to titanate-type structures has been elucidated. The reverse mechanism can be applied for the transformation of titanate to anatase. Ab initio molecular dynamics (ab-MD) calculations have been performed using the Harris functional and with the inclusion of both the Γ-point approximation and several *k*-points (Table 2). Three different size anatase wires with periodic conditions along the (0,1,0) direction were used as models.

It is found that the transformation mechanism, presented in Figure 10, involves the following sequential steps: (1) the anatase bulk is broken into small fragments (this might happen because of thermal fluctuations, stirring of the solution, and presence of NaOH). (2) A process of shifting and twisting of the atoms occurs in the [0,0,1] planes and along the (1,0,0) direction, which produces the oxygen atoms that are three-coordinated in anatase to get too close to the titanium atoms to form a bond (see Figure 10a−10c). (3) New Ti−O bonds are formed, and the involved oxygen atoms become four-coordinated forming the characteristic sequence of edge-sharing TiO_6 octahedrons of lepidocrocite-type titanate (see Figure 1b, 1d, and 1f or Figure 10d). (4) For the case of the largest system, it is observed that the edge-sharing TiO_6 octahedron layers are bonded forming a lepidocrocite-type bulk (Figure 1f or Figure 10d). For this particular case, simultaneously to the formation of the edge-

sharing TiO_6 octahedrons, there is a dislocation of the internal layer in the lepidocrocite-type bulk (Figure 10g) that eventually will yield lepidocrocite-type layers by the breaking of the elongated bonds. If there are defects during the formation of the edge-sharing TiO_6 octahedrons, then the formation of titanates of a given step would result. On the basis of these results, we conclude that the size of the initial anatase bulk is a determinant factor in the transformation and the final product.

Additionally, if step 1 titanate layers are formed, it is possible that they can be transformed into TiO_2 (B) because this structure is actually composed of a bulk structure of step 1 titanate, as shown in Figure 11g and 11h and in region 2 and region 3 of Figure 17. Finally, we consider that the mechanism for the formation of lepidocrocite−titanate layers (Figure 11f and Figure 10e) may be applied in a reverse path for the formation of anatase from titanate.

It is found that a very important factor on the transformation of the anatase-type sections to the characteristic sequence of edge-sharing TiO_6 octahedrons of titanates is the interaction of the $(0,0,\pm1)$ surfaces of the anatase with positive charges, which stress the surface deforming it and which promote the shifting-and-twisting mechanistic step (2) to take place. Experimentally, these charges are included in the solution as Na^+ or K^+ during the hydrothermal treatment. In the simulations presented in this work, we have modeled the presence of the positive charges either with sodium or hydrogen (theoretically cheaper to model), and they play the role of positive-prototype charges, which also ensure the electroneutrality of the system.

In the literature, there are several TiO_2 phases reported as the building block of the nanostructures obtained from the hydrothermal treatment of TiO_2 with NaOH (see Introduction). The atomic level mechanism found in this work can be used to explain the transformation from anatase to any of the published phases (lepidocrocite-type titanate, titanates of step 1 to step 3, and TiO_2 (B)), and the inverse mechanism can be applied to explain the transformation from laminar titanates and TiO_2 (B) to anatase.

Acknowledgment. The authors thank Dr. Marcelo Lozada-Cassou for fruitful and motivating discussions. This research has been supported under project D.00237.

CM062162L